LIQUID CRYSTALS, 1989, VOL. 4, NO. 3, 309–316

The influence of the flexoelectric effect on the electrohydrodynamic instability in nematics

by WOLFRAM THOM, WALTER ZIMMERMANN and LORENZ KRAMER
Physikalisches Institut der Universität Bayreuth, 8580 Bayreuth, F.R. Germany

(*Received 21 March 1988; accepted 20 September 1988*)

A rigorous three-dimensional linear analysis of the electrohydrodynamic instability in nematic liquid crystals including the flexoelectric effect is presented for the case of an applied d.c. voltage. The flexoelectric effect leads to an appreciable reduction of the threshold and to the appearance of oblique rolls at threshold for the standard material MBBA. We discuss the influence of a magnetic field and test several approximations against the rigorous results

The flexoelectric effect discovered by Meyer [1] induces for an applied electric field in a nematic or cholesteric slab novel phenomena [2–5]. The influence of the flexo-effect on the electrohydrodynamic instability was analysed only quite recently in a one dimensional model calculation [6] and it was suggested that the electrohydrodynamic oblique-roll convection structure [7–10] for the standard nematogen 4,-methoxybenzylidene-4′-*n*-butylaniline (MBBA) [11] is, for an applied d.c. voltage, induced by the flexo-effect. We show that these approximate analytical results are in qualitative agreement with our rigorous numerical calculations. Furthermore we investigate the influence of the strength of the flexoelectric effect as well as the influence of an external magnetic field on the oblique-roll structure. The assumption of a steady supercritical bifurcation leading to a stationary pattern above threshold, as observed [6], is made. Quantitative comparison with the experimental results of [6] is not possible since the material parameters of the compound used there are not known.

We consider a thin layer of a nematic liquid crystal of thickness d with the undistorted director $\hat{\mathbf{n}}$ parallel to the plates of the cell. The geometry is taken as in [8–10], i.e. the plates are chosen parallel to the xy plane at $z = \pm \pi/2$ (lengths are measured in units of d/π) with $\hat{n}$ parallel to the $\hat{x}$ direction and a d.c. voltage applied across the plates. Spherical polar coordinates are used to describe the director, so that for small deviations from the undistorted state $\hat{n} = (1, \psi, \theta)$. We start from the linearized equations of electrohydrodyamics (Equations (3.2) of [9]) for the angles θ and ψ, the induced electric potential ϕ and velocities v_x, v_y, v_z. The electric part of these equations consists of Poisson's and Ohm's laws with an anisotropic dielectric tensor and anisotropic conductivity. The dependence of all quantities on x and y can be chosen sinusoidal as before. To this system of equations we add the contributions of the flexoelectric effect as follows. In a distorted director field a flexoelectric polarization $\mathbf{P}$ is induced, given by [1, 12]

$$\mathbf{P} = e_1\hat{\mathbf{n}}(\operatorname{div}\hat{\mathbf{n}}) - e_3\hat{\mathbf{n}} \times (\operatorname{curl}\hat{\mathbf{n}}), \tag{1}$$

with the flexoelectric coefficients e_1 and e_3. As a consequence of Poisson's law the polarization produces contributions to the induced charge density $\varrho_{\text{flexo}} = -\operatorname{div}\mathbf{P}$ and to the free energy density $F_{\text{flexo}} = -\mathbf{E}\cdot\mathbf{P}$, where $\mathbf{E}$ is the (total) electric field.

The first effect causes a volume force $\varrho_{\text{flexo}} \cdot \mathbf{E}$ in the momentum balance equations, whereas the second effect contributes to the torque balance equations. Explicitly we then have to add to the y component of the torque the linear contribution (Equation (3.2 *b*) of [9])

$$-(e_1 + e_3)q\partial_z\phi - \frac{\sqrt{2}}{\pi}\bar{V}(e_1 - e_3)p\psi \tag{2a}$$

to the z component of the torque (Equation (3.2 *c*) of [9])

$$-\frac{\sqrt{2}}{\pi}\bar{V}(e_1 - e_3)p\theta + (e_1 + e_3)qp\phi \tag{2b}$$

and to the linear combination of the x and z component of the momentum equations (Equation (3.2 *e*) of [9])

$$-(e_1 + e_3)q^2\frac{\sqrt{2}}{\pi}\bar{V}(p\psi + \partial_z\theta) \tag{2c}$$

and we have to choose $\omega = \partial_t = 0$ for an applied d.c. field at threshold (for a complete form of the linear equations including the flexo-effect see [10]); q and p are the wavenumbers in the x and y direction. The terms proportional to $(e_1 - e_3)$ describe the coupling of an effective polarization with the electric field $\mathbf{E}$ and the terms proportional to $(e_1 + e_3)$ describe the electric quadrupole density that couples with the gradient $\nabla \cdot \mathbf{E}$ of the electric field [13].

The resulting set of six coupled ordinary differential equations in the variable z with the boundary conditions $\phi = \theta = \psi = v_x = v_y = v_z = 0$ at $z = \pm\pi/2$ has been solved both by numerical integration as well as by approximating the variables $\phi(z)$, $\theta(z)$, $\psi(z)$, $v_x(z)$, $v_y(z)$ and $v_z(z)$ by appropriate trial functions. Without the flexoelectric effect the lowest threshold voltage, V_c, is obtained if v_z, θ, ϕ are symmetric and v_x, v_y and ψ are antisymmetric with respect to the plane at $z = 0$ [8–10]. Including the flexoelectric terms the equations do not allow such a simple symmetry. We have therefore to superimpose functions of both types of symmetry as in the following two examples of trial functions;

$$\text{(1)} \quad (\phi, \theta, \psi, v_x, v_y) = (\phi^1, \theta^1, \psi^1, v_x^1, v_y^1)\cos(z) + (\phi^2, \theta^2, \psi^2, v_x^2, v_y^2)\sin(2z), \tag{3}$$

$$v_z = v_z^1\left[\frac{\cosh(\lambda z)}{\cosh[\lambda(\pi/2)]} - \frac{\cos(\lambda z)}{\cos[\lambda(\pi/2)]}\right] + v_z^2\left[\frac{\sinh(\lambda z)}{\sinh[\lambda(\pi/2)]} - \frac{\sin(\lambda z)}{\sin[\lambda(\pi/2)]}\right]. \tag{4}$$

Here v_z is a linear combination of Chandrasekhar functions [14].

$$\text{(2)} \quad (\phi, \theta, \psi, v_x, v_y) = (\phi^1, \theta^1, \psi^1, v_x^1, v_y^1)\left[\frac{\pi^2}{4} - z^2\right] + (\phi^2, \theta^2, \psi^2, v_x^2, v_y^2)\left(\frac{\pi^2}{4} - z^2\right)z, \tag{5}$$

$$v_z = v_z^1\left[\frac{\pi^2}{4} - z^2\right]^2 + v_z^2\left[\frac{\pi^2}{4} - z^2\right]^2 z. \tag{6}$$

These trial functions fulfil the boundary conditions. After inserting this ansatz into the linear equations and projecting the generalized Equations (3.2 *a–d*), (3.2 *f*) of [9] onto

$\cos(z)$ and $\sin(2z)$, or $[(\pi^2/4) - z^2]$ and $z\,[(\pi^2/4) - z^2]$, respectively, and equation (3.2 e) onto both Chandrasekhar functions or $[(\pi/4) - z^2]^2$ and $z\,[(\pi^2/4) - z^2]^2$, we obtain a fully algebraic system of equations for the twelve amplitudes.

In both cases, fully numerical solution and solution by trial functions, we obtain implicitly the neutral surface $V_0(q, p)$ from the solvability condition of the linear equations with boundary conditions. At $V = V_0(q, p)$ there is a steady bifurcation to a spatially periodic solution with wavevector (q, p). For the trial functions the solvability condition can be transformed into a cubic equation for V_0^2. For $q = 0$ only the flexoelectric terms proportional to $(e_1 - e_3)$ contribute (see Equations (2)) and the fully numerical solution goes over into the results for the non-convective periodic instability [2].

Inserting the standard values for the material parameters of MBBA [11] and the flexoelectric coefficients $(e_1 - e_3) = 4{\cdot}0 \times 10^{-12}$ Cb/m [15] and $(e_1 + e_3) = -2{\cdot}3 \times 10^{-11}$ Cb/m [16] the neutral surface $V_0(q, p)$ obtained by rigorous numerical solution of the linear equations has the absolute minimum $V_c = 4{\cdot}89$ V (threshold for the instability) at $q_c = 1{\cdot}25$ and $p_c = 1{\cdot}18$ corresponding to a tilt angle α ($\equiv$ arctan (p_c/q_c)) of 43·6°. For both approximations by trial functions the angle α is essentially unchanged but the wavenumber $\sqrt{(q_c^2 + p_c^2)}$ is, for the ansatz in Equations (3) and (4), about 3 per cent smaller and, for the ansatz in Equations (5) and (6), about 10 per cent smaller than the rigorous value of 1·72 ($1{\cdot}72\,\pi/d$ in dimensional units). The critical voltage V_c is essentially unchanged for the first ansatz and differs only slightly for the second ($V_c = 4{\cdot}8$ V). The threshold behaviour is independent of the thickness of the cell (voltage threshold), which is not strictly the case for an a.c. field [9, 10, 17]. The one dimensional model calculations of [6] are recovered when all z dependencies are neglected. With the assumption $(q_c^2 + p_c^2) = 1$ we then obtain for the material parameters used previously $V_c = 1{\cdot}7$ V and $\alpha = 51°$.

To demonstrate the strong influence of the flexoelectric effect on the threshold behaviour of the electrohydrodynamic instability under an applied d.c. voltage, we scale the two flexoelectric coefficients e_1, e_3 with a common factor ξ. For the given ratio $e_1/e_3 = 0{\cdot}71$ this allows us to show the dependence of the roll angle α and the critical voltage on the flexoelectric strength (see figure 1). α tends to 53° for large values of ξ. Beyond the critical value ξ_c of 0·21 oblique rolls have the lowest threshold V_c. The tilt angle α undergoes a pitchfork bifurcation at ξ_c ($\pm p$ symmetry). Without the flexoelectric effect ($\xi = 0$) the threshold voltage is higher, $V_c = 6{\cdot}4$ V, and the wavenumber smaller, $\sqrt{(q_c^2 + p_c^2)} = 1{\cdot}52$. In the table the influence of various changes of the coefficients e_1 and e_3 by up to about 20 per cent from their experimental values (first column) is exhibited. V_c and α are especially sensitive to variations of $(e_1 - e_3)$ keeping $(e_1 + e_3)$ fixed (compare the 1st, 6th and 7th columns). Note that in the table V_c always decreases with increasing α. For large values of ξ the angle α either tends to 90°, so that the instability becomes non-convective [2] or α tends to a value between 0° and 90°. The first case always occurs when $e_1 \approx -e_3$ whereas the second case always occurs when $e_1 \approx e_3$.

Without the flexo-effect the angle α increases with increasing values of $\sigma_\parallel/\sigma_\perp$ (> 1), that is the ratio of the conductivities parallel ($\sigma_\parallel$) and perpendicular ($\sigma_\perp$) to the director $\hat{\mathbf{n}}$. Including the flexo-effect we find that the angle α decreases from $\alpha = 44{\cdot}1°$ at $\sigma_\parallel/\sigma_\perp = 2$ slightly down to $\alpha = 43{\cdot}4°$ at $\sigma_\parallel/\sigma_\perp = 1{\cdot}57$ and then increases to a maximum $\alpha = 50°$ at $\sigma_\parallel/\sigma_\perp = 1{\cdot}02$. For smaller values of $\sigma_\parallel/\sigma_\perp$ α decreases again. The threshold voltage V_c always increases for decreasing $\sigma_\parallel/\sigma_\perp$ and diverges for $\sigma_\parallel/\sigma_\perp \to 1$ ($\varepsilon_a = \varepsilon_\parallel - \varepsilon_\perp < 0$). This means that the Carr–Helfrich mechanism, which

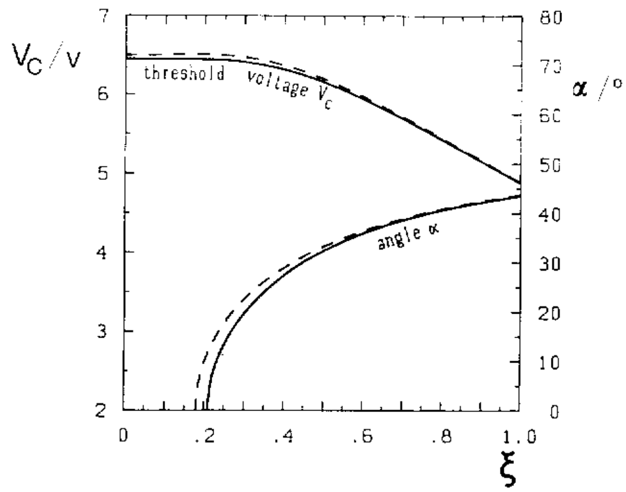

Figure 1. The threshold voltage V_c and the angle $\alpha = \text{arctg}(p_c/q_c)$ between the axis of the convection-rolls and the y axis are given as a function of the flexoelectric strength ξ (the flexoelectric coefficients are $e_1 = \xi(-0{\cdot}97) \times 10^{-11}\,\text{C}\,\text{b}\,\text{m}^{-1}$ and $e_3 = \xi(-1{\cdot}37) \times 10^{-11}\,\text{C}\,\text{b}\,\text{m}^{-1}$) for the rigorous numerical solution (solid curves) and for the trial functions given in equations (3) and (4) (dashed curves).

Threshold voltage V_c, angle α and wavenumber $\sqrt{(q_c^2 + p_c^2)}$ for different values of the flexoelectric coefficients e_1 and e_3.

$e_1/10^{-11}$ Cb m^{-1}	−0·97	−1·17	−0·77	−0·97	−0·97	−0·74	−1·20
$e_3/10^{-11}$ Cb m^{-1}	−1·37	−1·37	−1·37	−1·63	−1·10	−1·60	−1·14
V_c/V	4·89	5·25	4·50	4·06	5·73	3·74	5·94
α/degree	43·6	39·7	47·5	48·7	36·3	52·3	31·6
$\sqrt{(q_c^2 + p_c^2)}/d\pi^{-1}$	1·72	1·72	1·70	1·68	1·70	1·64	1·66

depends on a positive anisotropy of the conductivity, remains the driving force for the electrohydrodynamic instability. As in the case without the flexo-effect [8–10] the angle α always increases with increasing values of ε_a.

At $\varepsilon_a = 0{\cdot}49$ ($\sigma_\parallel/\sigma_\perp = 1{\cdot}5$) the threshold voltages for the non-convective periodic instability with $q = 0$ and $p_c = 0{\cdot}4$ and for the oblique-roll instability with $\alpha = 50°$ and $\sqrt{(q_c^2 + p_c^2)} = 1{\cdot}2$ become equal ($V_c = 3{\cdot}8$ V). For $\varepsilon_a > 0{\cdot}49$ the non-convective instability has the lower threshold. This situation, where two secondary patterns bifurcate simultaneously from a primary state, is a type of a codimension-2 bifurcation. As in the case without the flexoelectric effect [9, 10] the critical wavenumber p_c of the non-convective instability can be increased by appropriate changes of the material parameters (e.g. by lowering k_{22}/k_{11} [18]). Then the two minima of the neutral surface $V_0(q, p)$ coalesce and by varying ε_a or an external field we can go smoothly from the oblique-roll to the non-convective instability. Alternatively the critical wavenumber p_c of the non-convective instability can also be lowered, e.g. by a further increase of ε_a, until at $\varepsilon_a = 0{\cdot}73$ p_c reaches zero smoothly and thereby the instability goes over into the homogeneous Fréedericksz transition. By changing another parameter, e.g. $\sigma_\parallel/\sigma_\perp$, this degeneracy can even be made to happen at the same threshold as the oblique-roll instability, which then constitutes a kind of codimension-3 situation. With the parameters for MBBA it occurs at $\sigma_\parallel/\sigma_\perp = 2{\cdot}0$, $\varepsilon_a = 0{\cdot}73$, $V_c = 3{\cdot}2$ V, $\alpha = 50°$ and $\sqrt{(q_c^2 + p_c^2)} = 1{\cdot}2$.

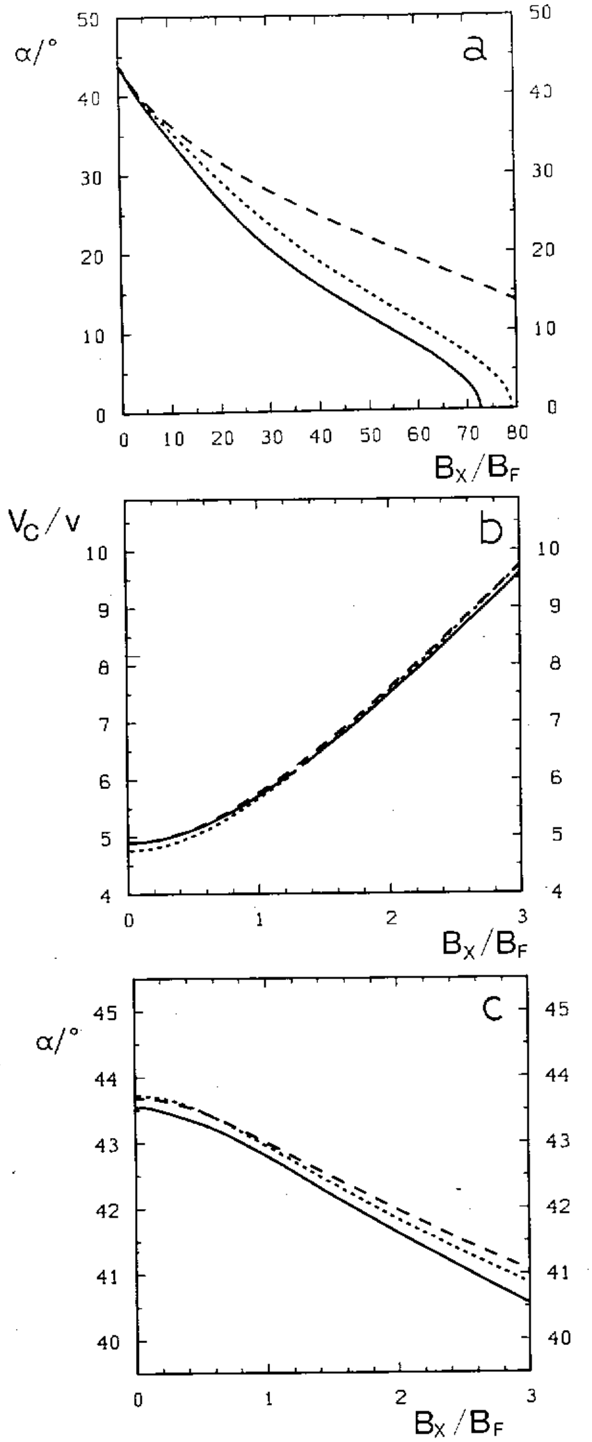

Figure 2. The dependence of the threshold voltage V_c (*b*) and the angle α (*a* and *c*) on a magnetic flux density B_x is shown (the magnetic anisotropy is assumed to be positive and B_F is the splay Freédericksz transition flux density). Solid curves: Rigorous numerical result, short-dashed curves: Trial functions from equations (5) and (6), long dashed curves: Trial functions from equations (3) and (4).

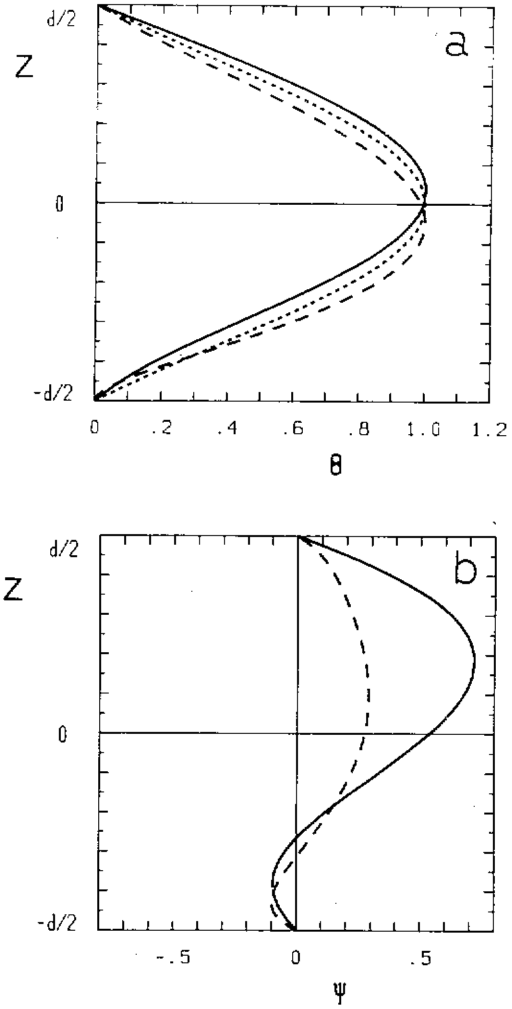

Figure 3. The z dependence of the angles θ (a) and ψ (b), describing the deviation of the director from the undistorted orientation are shown. The maximum of θ is normalized to 1. The solid curves are for zero applied magnetic field, the long-dashed curves for $B_x/B_F = 10$, and the short-dashed curves show the z dependence without flexoelectric effect and $B_x = 0$ (then normal rolls are obtained, so that $\psi = v_y = 0$).

For the oblique-roll structure there is a deflection of the director out of the xz plane ($\psi \neq 0$). This director deflection, and therefore the oblique-roll structure can be suppressed by a magnetic field in the x direction if the diamagnetic anisotropy $\chi_a = \chi_\parallel - \chi_\perp$ is positive (e.g. MBBA) or a magnetic field in the y direction for the rare case of negative χ_a. In the first case the θ deflection of the director is also suppressed and so the threshold voltage, V_c, and the wavenumbers also change considerably (see figure 2 (a)). To suppress the oblique-roll structure a fairly high magnetic flux density $B_x/B_F = 73$ is needed (B_F is the critical magnetic flux density for the splay Fréedericksz transition). The range of magnetic fields shown in figures 2 (b) and (c) should be experimentally easily accessible. The curvatures of $V_c(B_x)$ and $\alpha(B_x)$ at $B_x = 0$ are given by $B_F^2 d^2 V_c/dB_x^2 = 1{\cdot}91$ V and $B_F^2 d^2 \alpha/dB_x^2 = -1{\cdot}96°$. In the case of negative χ_a a much smaller magnetic field has to be applied in the y direction to suppress the oblique rolls ($B_x/B_F = 5{\cdot}5$ for MBBA parameters). The high magnetic flux density B_x ($\chi_a > 0$) to suppress oblique rolls is a consequence of the fact that the relevant terms, which are those proportional to $(e_1 - e_3) \cdot p$ in equations (2 *a*) and (2 *b*), are also proportional to $\bar{V}$. Thus B_x has antagonistic effects on these terms: on the one hand they are reduced because $|\theta|$ and $|\psi|$ are lowered and on the other they are increased because the threshold voltage rises.

In figure 3 the z dependences of the angles θ and ψ are plotted to give an impression of the influence of the flexoelectric effect on the convective state. We show results for zero applied magnetic field (solid), for $B_x/B_F = 10$ (long-dashed), and for zero field without flexoelectric effect (short-dashed; then normal rolls are obtained so that $\psi = v_y = 0$). Without the flexo-effect θ and v_z are symmetric and ψ, v_x and v_y are antisymmetric. These symmetries are disturbed only rather weakly except for ψ. As a consequence of the disturbed z symmetry the trajectories of fluid particles in oblique rolls are not closed, so that there is a spiraling motion. For particles near the roll axis we find trajectories on left-hand helices while the trajectories with diameter greater than about $d/2$ are right-hand spirals. However, in both cases the maximum pitch (that is the motion along the roll axis per revolution) is lower than $d/100$.

In conclusion we have shown, that for an applied d.c. voltage there is a considerable influence of the flexo-effect on the electrohydrodynamic instability which is in agreement with the earlier one dimensional calculations [6]. For an a.c. voltage the effect does not contribute to the well-known lowest-order frequency expansion (see e.g. [8, 9, 10, 17]). From this we should conclude that for not too thin layers with sufficiently high conductivity the flexoelectric effect has little influence in appropriate frequency ranges, which is in fact in agreement with rigorous numerical results [19]. When the lowest-order frequency expansion breaks down the threshold voltage becomes thickness dependent and the strict separation into a conduction and a dielectric regime is removed. In the oblique-roll regime a rectangular structure made up of a superposition of rolls having two degenerate orientations is, in principle, possible at threshold [20]. To decide on this possibility, which appears especially likely for roll-angles around 45°, a non-linear calculation is necessary.

After this paper had been submitted for publication we obtained a manuscript by Raghunathan and Madhusudana [21] on the same subject. The results of their computations agree with ours.

This work was supported by the Deutsche Forschungsgemeinschaft (Sonderforschungsbereich 213, Bayreuth) and the Emil-Warburg Stiftung (Bayreuth).

References

[1] Meyer, R. B., 1969, *Phys. Rev. Lett.*, **22**, 918.

[2] Bobylev, Yu. P., and Pikin, S. A., 1977, *Zh. eksp. teor. Fiz.*, **72**, 369 [1977, *Soviet Phys. JETP*, **45**, 195]. Barnik, M. I., Blinov, L. M., Trufanov, A. N., and Umanskii, B. A., 1977, *Zh. eksp. teor. Fiz.*, **73**, 1936 [1977, *Soviet Phys. JETP*, **46**, 1016].

[3] Chigrinov, V. V., Belyaev, V. V., Belyaev, S. V., and Grebenkin, M. F., 1977, *Zh. eksp. teor. Fiz.*, **77**, 2081 [1979, *Soviet Phys. JETP*, **50**, 994]. Umanskii, B. A., Chingrinov, V. G., Blinov, L. M., and Pod'yachev, Yu. B., 1981, *Zh. eksp. teor. Fiz.*, **81**, 1307 [1981, *Soviet Phys. JETP*, **54**, 694].

[4] Patel, J. S., and Meyer, R. B., 1987, *Phys. Rev. Lett.*, **58**, 1538.

[5] Barbero, G., Dozov, I., Palierne, J. F., and Durand, G., 1986, *Phys. Rev. Lett.*, **56**, 2056. Barbero, G., and Durand, G., 1987, *Phys. Rev.* A, **35**, 1294.

[6] Madhusudana, N. V., Raghunathan, V. A., and Sumathy, K. R., *Pramana J. Phys*, **28**, L311. There are some misprints in equations (5) and (7).

[7] Joets, A., and Ribotta, R., 1984, *Cellular Structures in Instabilities* edited by J. E. Wesfreid and S. Zaleski, (Springer), p. 294; 1986, *J. Phys., Paris*, **47**, 595. Ribotta, R., Joets, A., and Lei, Lin, 1986, *Phys. Rev. Lett.*, **56**, 1595.

[8] Zimmermann, W., and Kramer, L., 1985, *Phys. Rev. Lett.*, **55**, 402.

[9] Bodenschatz, E., Zimmermann, W., and Kramer, L., 1988, *J. Phys., Paris*, **49**, 1875.

[10] Zimmermann, W., 1987, Phd. thesis, Universitaet Bayreuth.

[11] Experimental values of the material constants for MBBA at 25°C: Elastic constants $k_{11} = 6{\cdot}66 \times 10^{-12}\,\mathrm{N}$, $k_{22} = 4{\cdot}2 \times 10^{-12}\,\mathrm{N}$ and $k_{33} = 8{\cdot}61 \times 10^{-12}\,\mathrm{N}$ are taken from de Jeu, W. H., Claassen, W. A. P., and Spruijt, A. M. J., 1976, *Molec. Crystals liq. Crystals*, **37**, 269. Viscosities $\alpha_1 = -18{\cdot}1 \times 10^{-3}\,\mathrm{kg\,m^{-1}\,s^{-1}}$, $\alpha_2 = -110{\cdot}4 \times 10^{-3}\,\mathrm{kg\,m^{-1}\,s^{-1}}$, $\alpha_3 = -1{\cdot}1 \times 10^{-3}\,\mathrm{kg\,m^{-1}\,s^{-1}}$, $\alpha_4 = 82{\cdot}6 \times 10^{-3}\,\mathrm{kg\,m^{-1}\,s^{-1}}$, $\alpha_5 = 77{\cdot}9 \times 10^{-3}\,\mathrm{kg\,m^{-1}\,s^{-1}}$, $\alpha_6 = -33{\cdot}6 \times 10^{-3}\,\mathrm{kg\,m^{-1}\,s^{-1}}$ are taken from Kneppe, H., Schneider, F., and Sharma, N. W., *J. chem. Phys.*, **77**, 3203. Unless stated otherwise we took $\varepsilon_a = -0{\cdot}53$ and $3\bar{\varepsilon} = (2\varepsilon + \varepsilon_{\|}) = 15{\cdot}22$ and the conductivity ratio $\sigma_{\|}/\sigma_{\perp} = 1{\cdot}5$ from: Diguet D., 1970, *C. r. hebd. Seanc. Acad. Sci.* **B**, **271**, 954.

[12] See also de Gennes, P. G., 1974, *The Physics of Liquid Crystals* (Clarendon Press).

[13] See, Durand, G., 1984, *Molec. Crystals liq. Crystals*, **113**, 237.

[14] Chandrasekhar, S., 1961, *Hydrodynamic and Hydromagnetic Stability* (Clarendon Press), p. 635.

[15] Dozov, I., Martinot-Lagarde, Ph., and Durand, G., 1982, *J. Phys., Paris*, **43**, L-365.

[16] Madhusudana, N. V., and Durand, G., 1985, *J. Phys., Paris*, **46**, L-195.

[17] Dubois-Violette, E., de Gennes, P. G., and Parodi, O., 1971, *J. Phys., Paris*, **32**, 305. Sengupta, P., and Saupe, A., 1974, *Phys. Rev.* A, **9**, 2698. Goossens, W. J. A., 1978, *Advances in Liquid Crystals*, Vol. 3, edited by G. H. Brown (Academic Press), p. 1.

[18] Lonberg, F., and Meyer, R. B., 1985, *Phys. Rev. Lett.*, **55**, 718. Miraldi, E., Oldano, C., and Strigazzi, A., 1986, *Phys. Rev.* A, **34**, 4348. Zimmermann, W., and Kramer, L., 1986, *Phys. Rev. Lett.*, **56**, 2655. Kini, U. D., 1986, *J. Phys., Paris*, **47**, 693.

[19] Zimmermann, W., and Thom, W. (in preparation).

[20] Pesch, W., and Kramer, L., 1986, *Z. Phys.* **B**, **63**, 121.

[21] Raghunathan, V. A., and Madhusudana, N. V., 1988, *Pramana J. Phys.*, **31**, L163.